Selected CR Features from Plasma Physics Perspective

Mikhail Malkov

UCSD

GSSI Workshop

Observations that seemingly contradict the SNR/DSA hypothesis of CR origin

1. "Pamela puzzle"- anomaly in He/p ratio:
   $\Delta q = 0.101 \pm 0.001$ in $\sim 10 - 100 \, GeV$ energy range of the CR background spectrum
2. Morphology of SNR sources, such as W44 (bipolar, not always correlated with molecular gas distribution)
3. Sharp anisotropy ($\sim 10°$) in the background spectrum in $10 \, TeV$ range, inconsistent with acceleration models
4. Brakes in the CR spectra around few GeV from SNR W44, IC 433, W51C
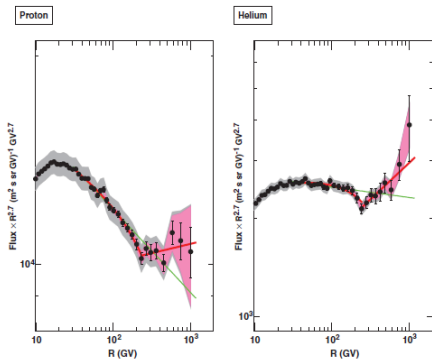
II. Pamela p/He anomaly

Fig. 4. Proton (left) and helium (right) spectra in the range 10 GV to 1.2 TV. The gray shaded area represents the estimated systematic uncertainty, and the pink shaded area represents the contribution due to tracker alignment. The green lines represent fits with a single power law in the rigidity range 30 to 240 GV. The red curves represent the fit with a rigidity-dependent power law (30 to 240 GV) and with a single power law above 240 GV.

- The PAMELA orbital telescope revealed deviation between helium and proton spectra deemed inconsistent with DSA, Adriani et al 2011

- points to initial phase of acceleration where elemental similarity does not apply

Pamela puzzle
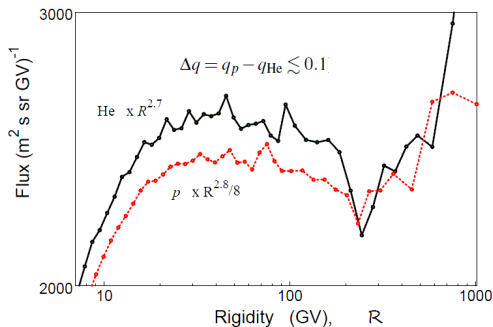
Salient features

$\Delta q = 0.101 \pm 0.001$ for $\mathscr{R} \gtrsim 5$ GV,

• almost identical (three digits in the indices) convex shapes at $5 < R < 230\text{-}240$ GV with a likely roll-over towards the right end of this interval

• sharp dip at $R = 230\text{-}240$ GV

• upturn with nearly the same slope at $R > 230\text{-}240$ GV.

Elemental invariance

Rigidity

$$\vec{\mathscr{R}} = \mathbf{p}c/eZ$$

Equations

$$\frac{1}{c}\frac{d\vec{\mathscr{R}}}{dt} = \mathbf{E}\left(\mathbf{r},t\right) + \frac{\vec{\mathscr{R}} \times \mathbf{B}\left(\mathbf{r},t\right)}{\sqrt{\mathscr{R}_0^2 + \mathscr{R}^2}}$$

$$\frac{1}{c}\frac{d\mathbf{r}}{dt} = \frac{\vec{\mathscr{R}}}{\sqrt{\mathscr{R}_0^2 + \mathscr{R}^2}}.$$

where

$$\mathscr{R}_0 = Am_p c^2/Ze,$$

Diffusive shock acceleration (DSA) mechanism predicts a power-law distribution for accelerated particles

$$\propto p^{-q}$$

where

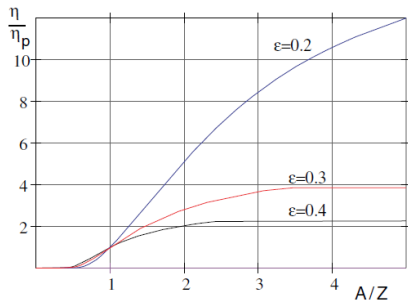$$q = 4/\left(1 - M^{-2}\right)$$

Suggested explanations

- Zatsepin & Sokolskaya (2006): three different types of accelerators contribute to the observed spectra
- Ohira & Ioka (2011): outward-decreasing helium abundance in certain SNR explosion sites, such as super-bubbles, may also result in harder helium spectra, as generated in stronger shocks
- Drury (2011): He is neutral in the ISM when it is processed by old and weak SNR shocks, and it is ionized when the SNRs are young and the shocks are strong
- Blasi & Amato 2011: spallation processes lead to deficiency of He at lower energies (longer confinement time in the Galaxy)
- Ptuskin & Zirakashvili (2012) p/He --Forward/reverse shock

❖ single shock propagating into *fully ionized homogeneous* ISM
   → suggested mechanisms cannot explain 0.1 difference in the slopes

➢ p/He spectral anomaly (if not explained) seriously undermines or even dismisses the DSA as a viable source of galactic CRs

26

Mach number

Collisionless plasma SNR shocks
(Sagdeev, 1979; Kennel et al., 1985;
Papadopoulos, 1985; MM, 1998)
inject more He2 when they are stronger
and so produce harder He spectra

injection bias is due to Alfven waves
driven by protons, so He2+ ions are
harder to trap by these waves because
of the larger gyroradii.

Downstream

Upstream

Suprathermal particle

B-field

Thermal,
Leaking particles
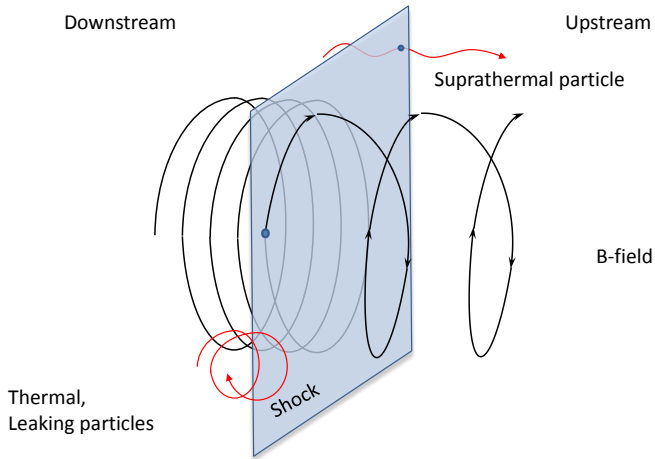
Shock

Physics of He preferential injection

Pitch-angle/gyro-phase plane downstream
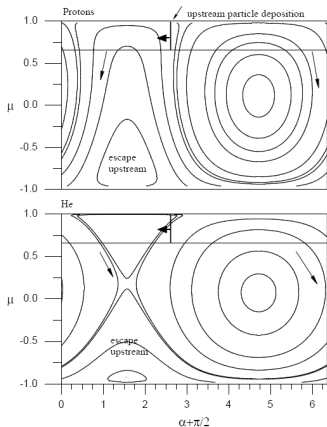
• upon crossing the shock, both protons and He randomize their downstream frame velocity (not energy)
• proton gyro-radius is a half of that of He2+ (for given velocity V_shock)
• He ions have better chances to return upstream since protons are retained by the downstream waves more efficiently.
• injection rates of both species decrease with the Alfven Mach but the proton injection decreases faster
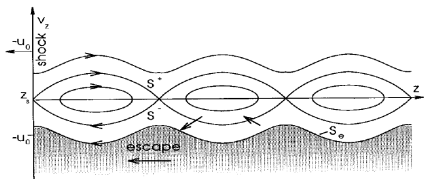
How does the He-biased injection translates into observed spectra?

- Injection scalings (MM, 1998):

$$\eta_p \approx 0.4 \cdot M_A^{-\sigma_p} \quad \text{with} \quad \sigma_p \approx 0.6.$$

$$\eta_{\text{He}} \approx 0.5 \cdot M_A^{-\sigma_{\text{He}}} \quad \text{with} \quad \sigma_{\text{He}} \approx 0.3$$
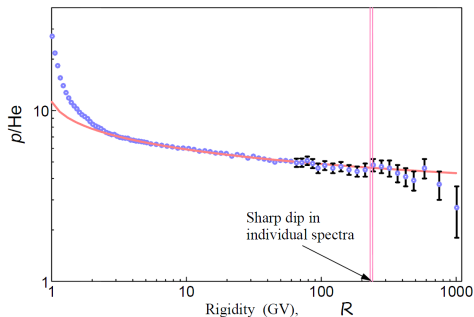
Contribution to the total number of CRs deposited inside the forward shock over the Sedov-Taylor SNR evolution phase:

$$N_\alpha(p) = A \int_{M_{\text{max}}^{-2}}^{M_{\text{min}}^{-2}} f_\alpha(p,M)\, dM^{-2}$$

$$f_\alpha \propto \eta_\alpha(M) \left(\mathscr{R}_{\text{inj}}/\mathscr{R}\right)^{q(M)}$$

Result

• take the ratio p/He, approximately:

$$N_p/N_{\mathrm{He}} \propto \left[\ln\left(\mathscr{R}/\mathscr{R}_{\mathrm{inj}}\right)\right]^{-(\sigma_p - \sigma_{\mathrm{He}})/2}$$
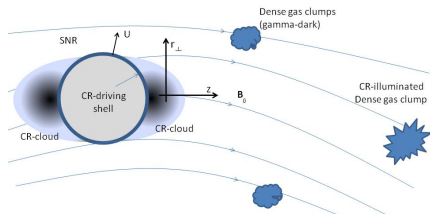
(from MM, P. Diamond,
R. Sagdeev 2012, PRL)

•heliospheric modulation not included

•higher rigidity end needs some adjustment of injection rates

Proton/Helium anomaly --- Summary

- the p/He ratio at ultrarelativistic rigidities, as opposed to the individual spectra, is not affected by the CR propagation, if collisions are negligible
- telltale signs, intrinsic to the particle acceleration mechanism
- reproducible theoretically with no free parameters
- collisionless shock theory needs to be advanced to predict the p/He ratio at higher rigidities (ATIC, CREAM, AMS-02)
- PIC simulations will be instrumental in computing p and He injection scalings with Mach number

CR escape along MF from two polar cusps of SNR

- CR diffuse along MF
- generate Alfvén waves that suppress diffusion
- to obtain CR distribution both processes are treated self-consistently
- result will determine MC emissivity

CR escape along MF from two polar cusps of SNR

- CR diffuse along MF
- generate Alfvén waves that suppress diffusion
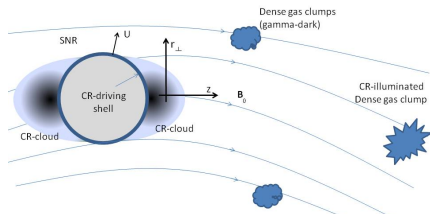- to obtain CR distribution both processes are treated self-consistently
- result will determine MC emissivity

CR escape along MF from two polar cusps of SNR

- CR diffuse along MF
- generate Alfvén waves that suppress diffusion
- to obtain CR distribution both processes are treated self-consistently
- result will determine MC emissivity

CR escape along MF from
two polar cusps of SNR

- CR diffuse along MF
- generate Alfvén waves that
  suppress diffusion
- to obtain CR distribution both
  processes are treated
  self-consistently
- result will determine MC
  emissivity

CR escape along MF from two polar cusps of SNR

- CR diffuse along MF
- generate Alfvén waves that suppress diffusion
- to obtain CR distribution both processes are treated self-consistently
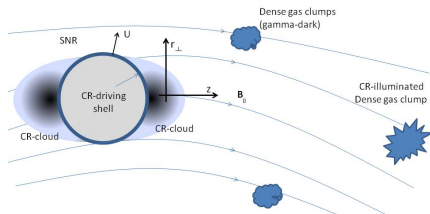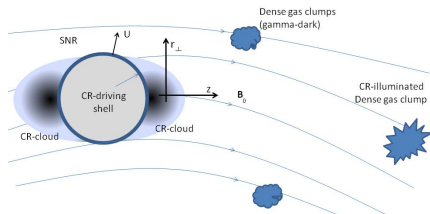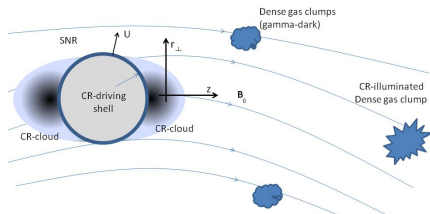- result will determine MC emissivity

- CR propagation in self-excited waves

$$\frac{d}{dt} P_{\mathrm{CR}}(p) = \frac{\partial}{\partial z} \frac{\kappa_{\mathrm{B}}}{I} \frac{\partial P_{\mathrm{CR}}}{\partial z}$$

$P_{\mathrm{CR}}(p)$ -partial pressure, $I(p)$ -wave energy, resonance $kp = eB_0/c$,
$d/dt = [\partial/\partial t + (U + C_{\mathrm{A}}) \partial/\partial z]$

- Wave generation by ∇P_{CR} associated with the CR pitch-angle anisotropy

$$\frac{d}{dt} I = -C_{\mathrm{A}} \frac{\partial P_{\mathrm{CR}}}{\partial z} - \Gamma I$$

- QL integral (Sagdeev et al '61)

$$P_{\mathrm{CR}}(z, t) = P_{\mathrm{CR0}}(z') - \frac{\kappa_{\mathrm{B}}}{C_{\mathrm{A}}} \frac{\partial}{\partial z} \ln \frac{I(z, t)}{I_0(z')}$$

$z' = z - (U + C_{\mathrm{A}}) t$

- CR propagation in self-excited waves

$$\frac{d}{dt}P_{\mathrm{CR}}(p) = \frac{\partial}{\partial z}\frac{\kappa_{\mathrm{B}}}{I}\frac{\partial P_{\mathrm{CR}}}{\partial z}$$

$P_{\mathrm{CR}}(p)$ -partial pressure, $I(p)$ -wave energy, resonance $kp = eB_0/c$,
$d/dt = [\partial/\partial t + (U + C_{\mathrm{A}})\partial/\partial z]$

- Wave generation by ∇P_{CR} associated with the CR pitch-angle anisotropy

$$\frac{d}{dt}I = -C_{\mathrm{A}}\frac{\partial P_{\mathrm{CR}}}{\partial z} - \Gamma I$$

- QL integral (Sagdeev et al '61)

$$P_{\mathrm{CR}}(z,t) = P_{\mathrm{CR}0}(z') - \frac{\kappa_{\mathrm{B}}}{C_{\mathrm{A}}}\frac{\partial}{\partial z}\ln\frac{I(z,t)}{I_0(z')}$$

$z' = z - (U + C_{\mathrm{A}})t$

- CR propagation in self-excited waves

$$\frac{d}{dt}P_{\mathrm{CR}}\left(p\right) = \frac{\partial}{\partial z}\frac{\kappa_{\mathrm{B}}}{I}\frac{\partial P_{\mathrm{CR}}}{\partial z}$$

$P_{\mathrm{CR}}\left(p\right)$ -partial pressure, $I\left(p\right)$ -wave energy, resonance $kp = eB_0/c$,
$d/dt = \left[\partial/\partial t + \left(U + C_{\mathrm{A}}\right)\partial/\partial z\right]$

- Wave generation by ∇P_{CR} associated with the CR pitch-angle anisotropy

$$\frac{d}{dt}I = -C_{\mathrm{A}}\frac{\partial P_{\mathrm{CR}}}{\partial z} - \Gamma I$$

- QL integral (Sagdeev et al '61)

$$P_{\mathrm{CR}}\left(z, t\right) = P_{\mathrm{CR0}}\left(z'\right) - \frac{\kappa_{\mathrm{B}}}{C_{\mathrm{A}}}\frac{\partial}{\partial z}\ln\frac{I\left(z, t\right)}{I_0\left(z'\right)}$$

$z' = z - \left(U + C_{\mathrm{A}}\right)t$

- CR/Alfven wave coupling

$$\frac{\partial W}{\partial t} - \frac{\partial}{\partial z}\frac{1}{W}\frac{\partial W}{\partial z} = -\frac{\partial}{\partial z}\mathcal{P}_0\left(z\right)$$

$W = \frac{C_A a(p)}{\kappa_B(p)}I$ -dimensionless wave energy, $d/dt \approx \partial/\partial t$, $\mathcal{P}_0$-initial CR distribution, $|z/a| < 1$

- Self-similar solution in variable $\zeta = z/\sqrt{t}$, $W\left(z, t\right) = w\left(\zeta\right)$ for $|z| > a$, outside initial CR cloud

$$\frac{d}{d\zeta}\frac{1}{w}\frac{dw}{d\zeta} + \frac{\zeta}{2}\frac{dw}{d\zeta} = 0$$

- solution depends on background turbulence level $W_0 \ll 1$, and on integrated CR pressure in the cloud:

$$\Pi = \int_0^1 \mathcal{P}_0 \, dz \gg 1$$

Reduction of Equations

- CR/Alfven wave coupling

$$\frac{\partial W}{\partial t} - \frac{\partial}{\partial z}\frac{1}{W}\frac{\partial W}{\partial z} = -\frac{\partial}{\partial z}\mathcal{P}_0\left(z\right)$$

$W = \frac{C_A a(p)}{\kappa_B(p)}I$ -dimensionless wave energy, $d/dt \approx \partial/\partial t$, $\mathcal{P}_0$-initial CR distribution, $|z/a| < 1$

- Self-similar solution in variable $\zeta = z/\sqrt{t}$, $W\left(z,t\right) = w\left(\zeta\right)$ for $|z| > a$, outside initial CR cloud

$$\frac{d}{d\zeta}\frac{1}{w}\frac{dw}{d\zeta} + \frac{\zeta}{2}\frac{dw}{d\zeta} = 0$$

- solution depends on background turbulence level $W_0 \ll 1$, and on integrated CR pressure in the cloud:

$$\Pi = \int_0^1 \mathcal{P}_0\, dz \gg 1$$

- CR/Alfven wave coupling

$$\frac{\partial W}{\partial t} - \frac{\partial}{\partial z}\frac{1}{W}\frac{\partial W}{\partial z} = -\frac{\partial}{\partial z}\mathcal{P}_0(z)$$

$W = \frac{C_A a(p)}{\kappa_B(p)}I$ -dimensionless wave energy, $d/dt \approx \partial/\partial t$, $\mathcal{P}_0$-initial CR distribution, $|z/a| < 1$
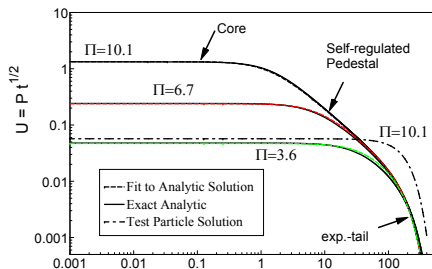
- Self-similar solution in variable $\zeta = z/\sqrt{t}$, $W(z,t) = w(\zeta)$ for $|z| > a$, outside initial CR cloud

$$\frac{d}{d\zeta}\frac{1}{w}\frac{dw}{d\zeta} + \frac{\zeta}{2}\frac{dw}{d\zeta} = 0$$

- solution depends on background turbulence level $W_0 \ll 1$, and on integrated CR pressure in the cloud:

$$\Pi = \int_0^1 \mathcal{P}_0\, dz \gg 1$$

Comparing and Contrasting with conventional TP predictions:

- considerable delay of CR escape
- narrower spatial distribution of CR cloud
- presence of extended self-similar, $\mathcal{P} \propto 1/z$ region

Self-confinement vs test-particle escape, $\sqrt{t}\mathcal{P}_{CR}$ vs $z/\sqrt{t}$ for different values of CR pressure Π (from MM, P. Diamond, R. Sagdeev, F. Aharonian and I. Moskalenko ApJ 2013)
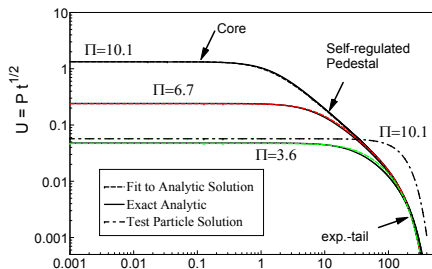
Comparing and Contrasting with conventional TP predictions:

- considerable delay of CR escape
- narrower spatial distribution of CR cloud
- presence of extended self-similar, $\mathcal{P} \propto 1/z$ region

Self-confinement vs test-particle escape, $\sqrt{t}\mathcal{P}_{CR}$ vs $z/\sqrt{t}$ for different values of CR pressure Π (from MM, P. Diamond, R. Sagdeev, F. Aharonian and I. Moskalenko ApJ 2013)
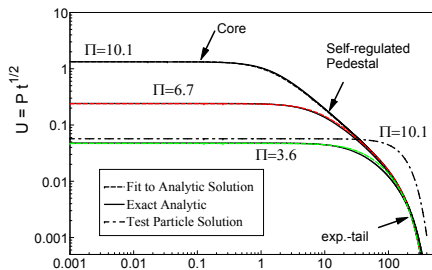
Comparing and Contrasting with conventional TP predictions:

- considerable delay of CR escape
- narrower spatial distribution of CR cloud
- presence of extended self-similar, $\mathcal{P} \propto 1/z$ region

Self-confinement vs test-particle escape, $\sqrt{t}\mathcal{P}_{CR}$ vs $z/\sqrt{t}$ for different values of CR pressure Π (from MM, P. Diamond, R. Sagdeev, F. Aharonian and I. Moskalenko ApJ 2013)

Comparing and Contrasting with conventional TP predictions:

- considerable delay of CR escape
- narrower spatial distribution of CR cloud
- presence of extended self-similar, $\mathcal{P} \propto 1/z$ region

Self-confinement vs test-particle escape, $\sqrt{t}\mathcal{P}_{CR}$ vs $z/\sqrt{t}$ for different values of CR pressure Π (from MM, P. Diamond, R. Sagdeev, F. Aharonian and I. Moskalenko ApJ 2013)
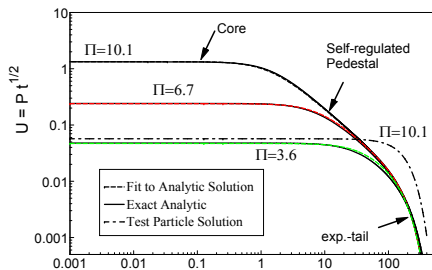
- CR partial pressure (found in closed but implicit form) is well approximated by:

$$\sqrt{t}\mathcal{P} = 2\left[\zeta^{5/3} + \left(D_{\mathrm{NL}}\right)^{5/6}\right]^{-3/5} e^{-W_0\zeta^2/4}$$

- particle diffusivity is strongly suppressed by **self-confinement** effect:

$$D_{\mathrm{NL}} = \frac{2}{V_0^2} D_{\mathrm{ISM}} e^{-\Pi}, \quad V_0 \sim 1$$

- as integrated CR pressure parameter is typically large:

$$\Pi \simeq 3\frac{C_{\mathrm{A}}}{c}\frac{a\left(p\right)}{r_{\mathrm{g}}\left(p\right)}\frac{\bar{P}_{\mathrm{CR}}\left(p\right)}{B_0^2/8\pi} \gg 1$$

- CR partial pressure (found in closed but implicit form) is well approximated by:

$$\sqrt{t}\,\mathcal{P} = 2\left[\zeta^{5/3} + (D_{\mathrm{NL}})^{5/6}\right]^{-3/5} e^{-W_0 \zeta^2/4}$$

- particle diffusivity is strongly suppressed by **self-confinement** effect:

$$D_{\mathrm{NL}} = \frac{2}{V_0^2} D_{\mathrm{ISM}} e^{-\Pi}, \quad V_0 \sim 1$$

- as integrated CR pressure parameter is typically large:

$$\Pi \simeq 3\frac{C_{\mathrm{A}}}{c}\frac{a\left(p\right)}{r_{\mathrm{g}}\left(p\right)}\frac{\bar{P}_{\mathrm{CR}}\left(p\right)}{B_0^2/8\pi} \gg 1$$

Results/CR pressure distribution

- CR partial pressure (found in closed but implicit form) is well approximated by:

$$\sqrt{t}\mathcal{P} = 2\left[\zeta^{5/3} + (D_{\mathrm{NL}})^{5/6}\right]^{-3/5} e^{-W_0\zeta^2/4}$$

- particle diffusivity is strongly suppressed by **self-confinement** effect:

$$D_{\mathrm{NL}} = \frac{2}{V_0^2} D_{\mathrm{ISM}} e^{-\Pi}, \quad V_0 \sim 1$$
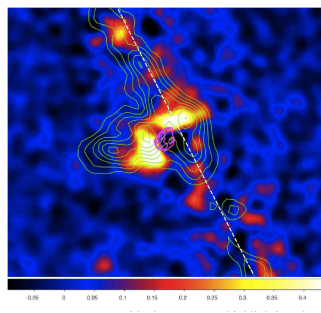
- as integrated CR pressure parameter is typically large:

$$\Pi \simeq 3 \frac{C_{\mathrm{A}}}{c} \frac{a\left(p\right)}{r_{\mathrm{g}}\left(p\right)} \frac{\bar{P}_{\mathrm{CR}}\left(p\right)}{B_0^2/8\pi} \gg 1$$

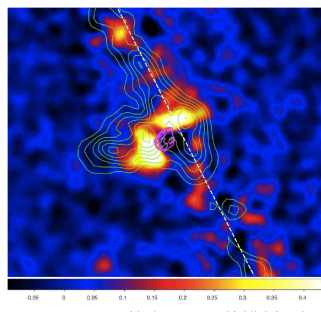- normalized partial pressure $\mathcal{P}(p)$ approximation

$$\mathcal{P} \approx 2 \left\{ z^{5/3} + [D_{\mathrm{NL}}(p)\, t]^{5/6} \right\}^{-3/5}$$

- for $D_{\mathrm{NL}}(p) < z^2/t$ momentum independent (DSA TP $f \sim p^{-4}$)
- at $p = p_{\mathrm{br}}$, $D_{\mathrm{NL}}(p_{\mathrm{br}}) = z^2/t$, $D_{\mathrm{NL}} \propto p^{\delta}$, break index $= \delta/2$
- δ from $D_{\mathrm{ISM}}(p)$ and CR pressure $\Pi(p)$
- if $\exp(-\Pi) \propto p^{-\sigma}$ and $D_{\mathrm{ISM}} \propto p^{\lambda}$ at $p \sim p_{\mathrm{br}}$, so $\delta = \lambda - \sigma$, then
- $\mathcal{P}$ is flat at $p < p_{\mathrm{br}}$ for $\delta > 0$ and steepens to $p^{-\delta/2}$ at $p = p_{\mathrm{br}}$.
- if $\delta < 0$, $\mathcal{P}$ raises with p as $p^{-\delta/2}$ at $p < p_{\mathrm{br}}$ and it levels off at $p > p_{\mathrm{br}}$

Fermi-LAT γ-image of SNR W44, *Uchiyama et al 2012*

- central source (magenta radio image) emission is masked
- bi-polar morphology of escaping CR is clearly seen
- not everywhere correlated with the dense gas (green contours) distribution: strong γ-flux is expected from overlapping regions of CR and gas density
- strong indication of field aligned propagation
- various analyzes of various sources (*e.g. Uchiyama et al 2012)* indicate that CR diffusivity is suppressed by up to a factor of ten

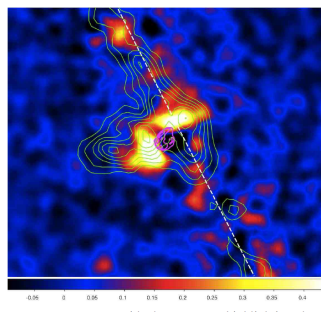Fermi-LAT γ-image of SNR W44, *Uchiyama et al 2012*

- central source (magenta radio image) emission is masked
- bi-polar morphology of escaping CR is clearly seen
- not everywhere correlated with the dense gas (green contours) distribution: strong γ-flux is expected from overlapping regions of CR and gas density
- strong indication of field aligned propagation
- various analyzes of various sources (*e.g. Uchiyama et al 2012*) indicate that CR diffusivity is suppressed by up to a factor of ten
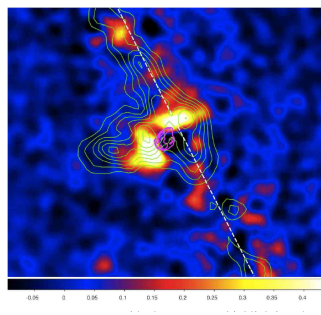
Fermi-LAT γ-image of SNR W44, *Uchiyama et al 2012*

- central source (magenta radio image) emission is masked
- bi-polar morphology of escaping CR is clearly seen
- not everywhere correlated with the dense gas (green contours) distribution: strong γ-flux is expected from overlapping regions of CR and gas density
- strong indication of field aligned propagation
- various analyzes of various sources (*e.g. Uchiyama et al 2012*) indicate that CR diffusivity is suppressed by up to a factor of ten
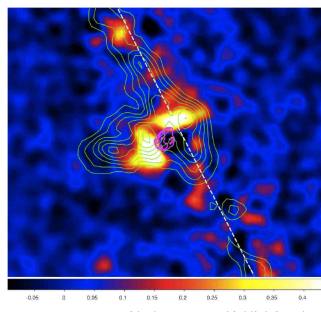
Fermi-LAT γ-image of SNR W44, *Uchiyama et al 2012*

- central source (magenta radio image) emission is masked
- bi-polar morphology of escaping CR is clearly seen
- not everywhere correlated with the dense gas (green contours) distribution: strong γ-flux is expected from overlapping regions of CR and gas density
- strong indication of field aligned propagation
- various analyzes of various sources (*e.g. Uchiyama et al 2012*) indicate that CR diffusivity is suppressed by up to a factor of ten
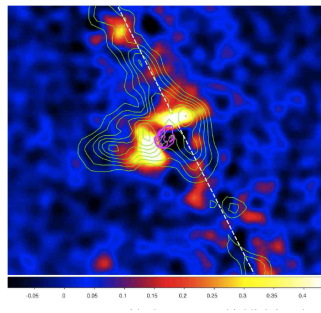
Fermi-LAT γ-image of SNR W44, *Uchiyama et al 2012*

- central source (magenta radio image) emission is masked
- bi-polar morphology of escaping CR is clearly seen
- not everywhere correlated with the dense gas (green contours) distribution: strong γ-flux is expected from overlapping regions of CR and gas density
- strong indication of field aligned propagation
- various analyzes of various sources (*e.g. Uchiyama et al 2012)* indicate that CR diffusivity is suppressed by up to a factor of ten

Fermi-LAT γ-image of SNR W44, *Uchiyama et al 2012*

- central source (magenta radio image) emission is masked
- bi-polar morphology of escaping CR is clearly seen
- not everywhere correlated with the dense gas (green contours) distribution: strong γ-flux is expected from overlapping regions of CR and gas density
- strong indication of field aligned propagation
- various analyzes of various sources (*e.g. Uchiyama et al 2012*) indicate that CR diffusivity is suppressed by up to a factor of ten

- escape of CR from their acceleration site is treated **self-consistently with self-generated Alfven waves using QL theory**
- resulting CR distribution is obtained in closed form
- strong **self-confinement** of escaping CR is demonstrated
- results are consistent with recent observations of W44 by *Fermi*-LAT
- escape spectra are roughly DSA-like power laws

I. Why study spectral breaks?

❖ ***instrumental in telling electron- from proton-gamma-emission***

➢ do we really see the proton (i.e., the primary CR component) emission

or just radiatively more efficient electrons generate the observed spectrum?

➢ test particle version of the DSA (power-law E^{-2} particle energy distribution, modulo propagation losses) reproduces the form of the energy spectrum reasonably well, BUT:

➢ a somewhat steeper power-law may better accommodate the $E^{-2.7}$ measured spectrum (even more so for NL ~1.5 very hard spectrum)

➢ direct observations of emission coming from particles accelerated in SNR shocks often indicate significantly steeper than E^{-2} spectra

➢ Spectral Breaks are observed (e.g. FERMI)

✓ interesting (plasma) physics of spectral breaks

Long standing community paradigm for SNR emission:

✓ power-law spectrum of parent particles (i.e. DSA generated, roughly E^-2)

✓ exponential cut-off (particle losses, limited acceleration time), e.g., Drury, Aharonian and Voelk, '94

▪ while plausible overall, fails in some cases:
e.g., search campaign for the TeV emission from a number of SNRs
- negative (Buckley et al 1998)
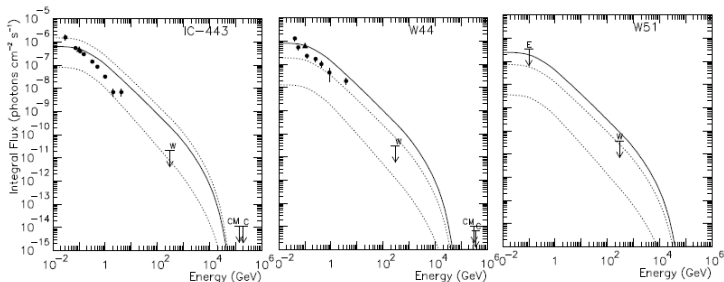
Observations of spectral breaks

- Spectral break around a few GeV detected by Fermi-LAT (Abdo et al 2009-2011: W44, IC443, W28, W51C)

- SB found consistent (along with the cut-off) with RXJ 1713 HESS data (Aharonian et al 2006), W51C

- anticipated by MM, Diamond and Sagdeev (2005) in RXJ 1713 analysis, mechanism suggested

- If SB was included in gamma-emission estimates (Drury et al94; Buckley 98), non-detection of TeV photons from some of the remnants (e.g., W44, IC443, W51) by IACTs would be no surprise

# Key element of spectrum steepening (break): wave-particle interaction in the foreshock plasma

- waves in strongly ionized (closer to the shock) medium propagate freely in a broad frequency range at the Alfven speed
  $$\omega = kV_A.$$

- When ion-neutral collision frequency is higher (deeper into the cloud), neutrals are entrained by the waves which are still able to propagate with a $\sqrt{\rho_i/\rho_0} < 1$ lower speed

- between these two regimes Alfven waves are heavily damped and even disappear altogether for sufficiently small $\rho_i/\rho_0 \ll 0.1$
  Kulsrud & Pearce '69; Zweibel & Shull '82

- evanescence wave number range is then bounded by

$$k_1 = v_{in}/2V_A \quad \text{and} \quad k_2 = 2\sqrt{\rho_i/\rho_0}\, v_{in}/V_A$$

spectrum steepening cont'd

- cyclotron resonance condition $kp_\parallel/m = \pm\omega_c$
- frequency range where the waves cannot propagate translates into the parallel momentum range

$$p_1 < |p_\parallel| < p_2$$
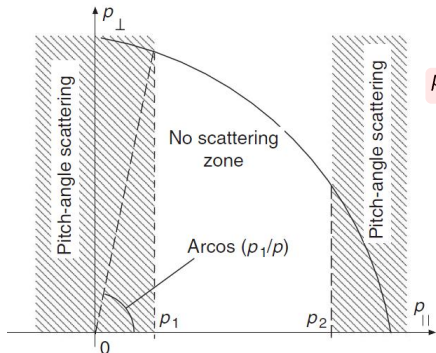
$p_1 = 2V_A m\omega_c/v_{in}, \quad p_2 = \dfrac{p_1}{4}\sqrt{\rho_0/\rho_i} > p_1$

➢ spectral break must form at the photon energy corresponding to the particle momentum

$$p = p_1 \equiv p_{br}$$

spectrum break cont'd

➤ locally isotropic component of new proton distribution (effective phase space dimension of emitting particles is reduced by one):

$$\overline{f}(p) = \int\limits_{0}^{\mu_1} f_0(p)\,d\mu = \begin{cases} (p_1/p)\,f_0(p), & p \geq p_1 \\ f_0(p), & p < p_1 \end{cases}$$

$$\mu_1 = \min\{p_1/p, 1\}$$

➤ slope of the particle momentum distribution becomes steeper by exactly one power above

$$p = p_1 \equiv p_{br}$$

➤ any power-law distribution $\propto p^{-q}$ upon entering an MC, turns into

$$p^{-q-1} \text{ at } p \geq p_{br}$$

Position of the break in the particle spectrum

-can be calculated using $\qquad p_1 = 2 V_A m \omega_c / \nu_{in}$

and i-n collision frequency (e.g., Draine and McKee 93, Drury et al 96)

<u>break momentum:</u>

- depends on the magnetic field strength
- ion density
- frequency of ion-neutral collisions
- ionization rate

$$\boxed{p_{br}/mc \simeq 10 B_\mu^2 T_4^{-0.4} n_0^{-1} n_i^{-1/2}}$$

❑ SNR W44: break in the photon spectrum is observed at about 2 GeV, which places the break on the proton distribution at about 7GeV/c

❑ constraints the above combination of parameters

Case Study W44: Acceleration model and proton spectrum

- need to determine the degree of nonlinear (NL) modification of the shock structure
- can be calculated self-consistently, given the shock parameters and the particle maximum momentum P_{max}
- in the case of a broken spectrum, P_{br} has the role of P_{max}
- in cases of low maximum momentum, the shock modification is weak, so the spectrum is more likely to be in the only slightly NL, almost test particle (TP) regime
- hint from radio observations (Castelletti et al, '07) : q=1.75
- calculate both NL and TP regimes

Gamma-ray emission spectrum SNR W44
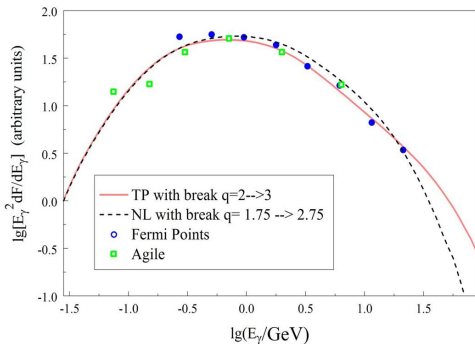
-Circles: Fermi-LAT, Abdo et al, 2010

-solid line: TP with break q=2→3, no cut-off to be specified to fit the data

-dashed line: NL DSA spectrum with break, requires cut-off at 300 GeV to fit; MM, P. Diamond, R. Sagdeev, 2011, Nature Comm.

-NB: only one decade in energy, higher fit quality

- Δq < 1 would require tweaking MC filling factor (e.g. W51C, Carmona talk, MAGIC)

Breaks: Conclusions

- ❖ recent observations of supernova remnant W44, W28, IC443 and W51C by Fermi-LAT indicate breaks in photon spectra and support the idea that the bulk of galactic cosmic rays is accelerated in SNRs by diffusive shock acceleration

- ❖ when a SNR expands into weakly ionized dense gas, significant revision of the mechanism is required

- ❖ strong ion-neutral collisions in the remnant surrounding lead to the steepening of the energy spectrum of accelerated particles by **exactly one power** (less if MC filling factor is low)

- ❖ gamma-ray spectrum generated in collisions of the accelerated protons with the ambient gas is calculated and successfully fitted to the Fermi-LAT data